Highly Aligned Scalable Platinum-decorated Single-wall Carbon Nanotube Arrays for Nanoscale Electrical Interconnects

Young Lae Kim *et al.*

Supporting Information

1. Detailed study of the alignment of SWNT architectures:

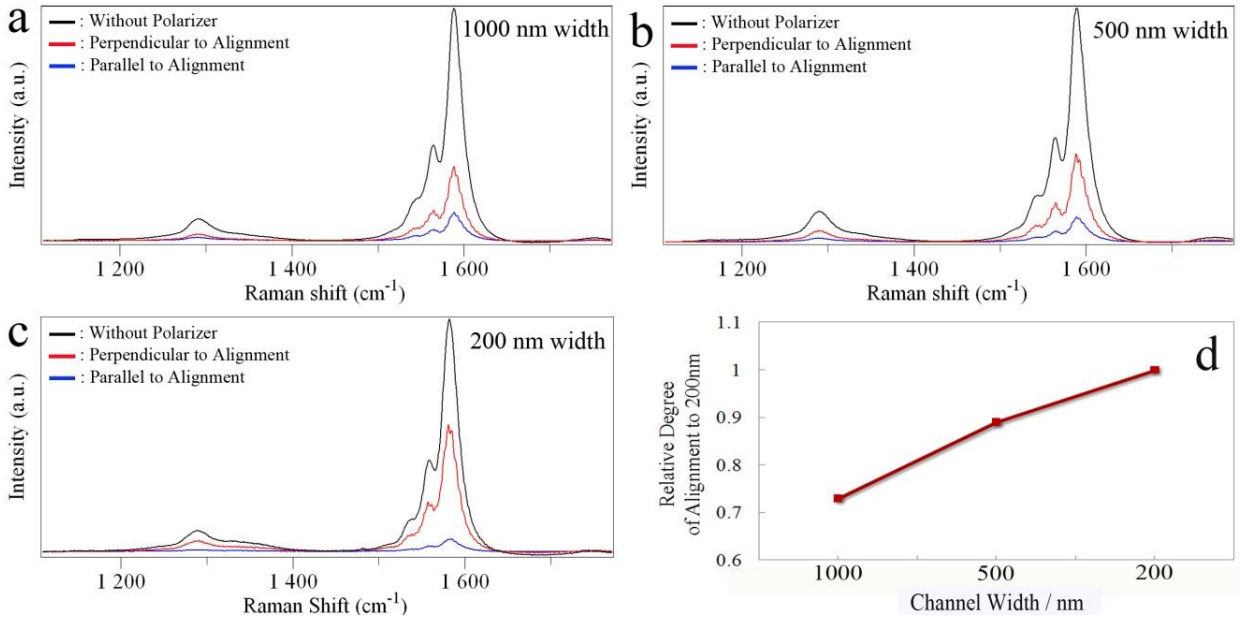

Figure S1. Polarized Raman spectra from highly organized SWNT arrays recorded with 785 nm wavelength laser. a) Tangential modes of 1000 nm width SWNTs channel. b) Tangential modes of 500 nm width SWNTs channel. c) Tangential modes of 200 nm width SWNTs channel. As channel width decrease from 1000 nm to 200 nm, the intensities of parallel-polarized tangential modes decrease and that of the perpendicularly polarized tangential modes increase. d) Degree of alignment of the SWNT arrays of different channel widths, relative to the degree of alignment of the 200 nm SWNT array.

Polarized Raman spectroscopy has been used in the past to study the symmetry of the vibrational modes of carbon nanotubes[S1]. Using this technique, past workers have reported study of SWNT alignment[S2] in fibers. In particular, the tangential modes give rise to a number of Raman active peaks at positions between 1550 cm^{-1} – 1610 cm^{-1}. By changing the polarization of the Raman Laser with respect to the alignment direction of our arrays, and noting the relative intensities of

the largest tangential peak (with respect to the intensity of the same peak in an unpolarized Raman spectrum), it is possible to quantify the degree of alignment of our SWNT arrays.

Highly organized and aligned SWNTs arrays in the nano structures were confirmed by polarized Raman spectroscopy. Figure S1a, S1b and S1c shows the tangential modes of aligned SWNT recorded using a micro Raman spectrometer with excitation wavelength of 785 nm. Each spectrum represents 60 accumulations each having an exposure time of 2s/spectrum. A 600 gr/mm grating was used, and the confocal hole diameter was set to 200 μm. In the polarized Raman experiments, half-wave plates were inserted allowing the rotation of the incident and scattered polarizations. The tangential modes of highly organized aligned SWNTs arrays were recorded using the VV configuration (same polarization for the incident and scattered light).[S1,S2] The parallel polarized intensities of the SWNTs arrays tangential mode (90° - shown with a blue line) decreased as the SWNTs channel width decreases from 1000 nm to 200 nm (S1a to S1c). On the other hand, it is clearly seen that, as the size of SWNTs array decreases from 1000nm to 200 nm (S1a to S1c), the perpendicular polarized intensities of tangential mode (0°, red line) increase. Figure S1d shows the relative degree of alignment of aligned SWNTs arrays (1000 nm, 500 nm and 200 nm), the degree of alignment calculated by ratio of the relative polarized Raman intensities of SWNT arrays (at 1583 cm^{-1}) with respect to that of the 200 nm SWNTs array since G band intensity is directly related to the in-plane graphitic structure. We find that the degree of alignment increase as the array width decrease from 1000 nm to 200 nm.

2. Details of band gap and conductance calculations:

Our calculations are based the first principle density functional method. In particular, we have used generalized gradient corrected approximation (GGA) of Perdew and Wang (PW91)[S3] for exchange and correlation functional. The calculations are based on super cell approach and the wave functions are expanded in plane waves. The ionic cores are replaced by ultrasoft pseudopotentials [S4]. We have used an energy cutoff of 400eV and Monkhorst-pack scheme for k-points sampling. The total energy is converged to within 0.01 meV. The calculations are carried out using VASP code[S5]. Specifically, the band structure and DoS were calculated for all the values of n ($0<n<13$) for three nanotubes of similar diameters, [8,0], [9,0], and [10,0]. The [8,0]

and [10,0] nanotubes are semiconducting defined by the indexing x-y=3m-1 and 3m+1 respectively, whereas the (9,0) tube is metallic with an indexing of x-y=3m, with m=3.

Detailed geometry optimized structures, electronic band structures and density of states (DoS) will be reported elsewhere. Here we summarize the most important and relevant findings:

1. Geometry optimization of atom-by-atom deposition of Pt on SWNT sidewalls appear to indicate that cluster formation at each site lowers the overall energy of the system in comparison to Pt-atoms wetting the sidewalls of the nanotube and forming films. This preference for cluster formation was in complete agreement with our experimental finding.

2. Addition of Pt atoms to these clusters caused significant charge transfer to the nanotubes, which gave rise to increasing number of new bands and increased DoS near the Fermi level of the nanotubes.

3. The increased number of bands near the Fermi level decreases the band-gap of semiconducting nanotubes.

4. The band gap of metallic nanotubes remain close or equal to zero for n=3 Pt atoms per cluster.

From the band structure and position of the band with respect to the Fermi level, we can calculate the zero bias conductance taking into account all contributing subbands near the Fermi level (both for electrons and holes). The total zero-bias conductance is given by,

$$G = \sum_{n_e} \frac{G_0}{1+\exp\{(+E^e_{\min}-E_f)/(k_BT/e)\}} + \sum_{n_h} G_0 \left(1 - \frac{1}{1+\exp\{(-E^h_{\max}-E_f)/(k_BT/e)\}}\right),$$

where G_0 is the quantum conductance, $2e^2/h \approx 1/(12.9\ \mathrm{k}\Omega)$, and $E^e_{\min}$ and $E^h_{\max}$ are the minimum and maximum energies of the conduction (electronic) subbands and valence (hole) subbands respectively. E_f is the Fermi level and the summing indices n_e and n_h correspond to the conduction and valence subbands. We note that for carbon nanotubes, each of these subbands are two-fold degenerate, such that a metallic nanotubes with no band gaps (i.e. either if $E^e_{\min}$ and $E^h_{\max} = E_f$, or if the bands go across the Fermi level), $G=4e^2/h$.

For all three n-Pt-SWNTs, the total conductance from all contributing bands was obtained using this equation, by using the energy minima/maxima obtained from our DFT calculations of the band structure. For convenience, the contribution from only those subbands was added that provides at least 1% of G_0 to the total conductance (the nearest subbands which are comparable to $k_BT \approx 0.026$ eV). The contribution of the next-nearest subbands falls sharply as they are further away from the Fermi level, with contributions for a separation of 0.1 eV becoming almost negligible. Despite this, for certain values of n, the conductance does exceed the value of $4e^2/h$, which is indeed a novel result for carbon nanotubes. Following the pattern of the band gap *vs.* n, the conductance occassionally falls below the $4e^2/h$ limit in the semiconducting nanotubes.

References for supporting information:

S1. Fantini, C.; Pimenta, M. A.; Dantas, M. S. S.; Ugarte, D.; Rao, A. M.; Jorio, A.; Dresselhaus, G.; Dresselhaus, M. S., Micro-Raman investigation of aligned single-wall carbon nanotubes. *Phys. Rev. B* **2001,** *63*, 161405(R)

S2. Gommans, H. H.; Alldredge, J. W.; Tashiro, H.; Park, J.; Magnuson, J.; Rinzler, A. G., Fibers of aligned single-walled carbon nanotubes: Polarized Raman spectroscopy. *J. Appl. Phys.* **2000,** *88*, (5), 2509-2514

S3. Perdew, J.P.; Chevary, J. A.; Vosko, S. H.; Jackson, K.A.; Perderson, M. R.; Singh, D.J.; Fiolhais, C., Atoms, molecules, solids, and surfaces: Applications of the generalized gradient approximation for exchange and correlation. *Phys. Rev. B*, **1992,** *46*, 6671-6687

S4. Vanderbilt, D., Soft self-consistent pseudopotentials in a generalized eigenvalue formalism. *Phys. Rev. B*, **1990,** *41*, 7892-7895

S5. Kresse, G.; Hafner, J., Ab initio molecular dynamics for liquid metals. *Phys. Rev. B*, **1993**, *47*, 558-561